

The Path Integrals of LF/VLF Wave Hop Theory

Leslie A. Berry and Mary E. Chrisman

Central Radio Propagation Laboratory, National Bureau of Standards, Boulder, Colo.

(Received June 10, 1965)

This paper continues development of a full wave propagation theory for low-frequency radio waves which is analogous to geometric optics. The effects of earth conductivity, reflection height, and earth curvature are described by the path integral, and accurate methods for computing it, especially suitable for a programmed computer, are given. Knowledge of the path integral and the ionospheric reflection coefficient, which are independent, permit calculation of skywave field strengths. Sample calculations are shown which confirm that the LF skywave is diffracted deep into the shadow region. Possible applications include calculation of LF and VLF field strengths and extraction of ionospheric reflection coefficients from field measurements.

1. Introduction

The full wave solution for propagation between a spherical earth and a concentric ionosphere can be expanded into a series of complex integrals. If the integrals are replaced by their saddle point approximations, the series is identified as the ray hop series of geometric optics, so the integrals are called wave hops [Berry, 1964]. This expansion was suggested by Rydbeck [1944] and Bremmer [1949]. Wait [1961] firmly established the connection with the ray hops, pointed out that the saddle point approximation was inadequate near, and beyond, the caustic, and suggested evaluating the wave hops by numerical integration or by summing a residue series. Wait and Conda [1961] made a few preliminary calculations. Continuing and extending this work, Berry [1964] included height gain formulas and calculated the wave hops by numerical integration for several representative cases.

A convenient form of the wave hops series is

$$E_r = E_0 + \sum_{j=1}^{\infty} \gamma_j I_j, \quad (1)$$

where E_0 is the groundwave and γ_j is an effective ionospheric reflection coefficient. For a locally plane isotropic ionosphere,

$$\gamma_j = T^j, \quad (2)$$

where T is the Fresnel reflection coefficient. The effects of ground conductivity, reflection height, earth curvature, and distance are accounted for by the path integral, I_j . This paper is concerned with calculation of the path integrals.

Section 2 describes in detail methods for calculating the path integrals for a wide range of frequency and distance. Some sample calculations are discussed in section 3, and two possible applications are discussed in section 4.

2. Path Integral Formulas

A vertical electric dipole source of waves with wave number $k = 2\pi/\lambda$ is on a spherical earth of radius a . A time function, $\exp(i\omega t)$, is assumed, and suppressed. The field is to be found on the surface at a distance $d = a\theta$. The effective reflection height is h .

For this paper, the starting point is equation (22) of Berry [1964]. Fock's [1946] approximations

for the spherical Hankel functions are

$$\zeta_{\nu-\frac{1}{2}}^{(1)}(x) \cong -i \left(\frac{x}{2}\right)^{1/6} W_2(t), \quad (3a)$$

and

$$\zeta_{\nu-\frac{1}{2}}^{(2)}(x) \cong i \left(\frac{x}{2}\right)^{1/6} W_1(t), \quad t = \left(\frac{2}{x}\right)^{1/3} (\nu - x). \quad (3b)$$

The Airy functions $W_k(x)$ are discussed by Spies and Wait [1961]. Using (3), and the asymptotic form for the Legendre function, $P_\nu(\cos \theta)$, the path integral for the j th wave hop is

$$I_j \cong e^{-i3\pi/4} K \frac{e^{-ikd}}{\sqrt{\sin \theta}} \int_{\Gamma} (1+zt)^{5/2} e^{-ixt} W_1(t) W_2(t) (1+R_e(t))^2 R_e^{j-1}(t) p^j(t) dt, \quad (4)$$

where $x = v\theta$, $y = kh/v$, $z = 0.5/v^2$, $v = \left(\frac{ka}{2}\right)^{1/3}$, and (5)

Γ is the contour of integration described below. The ground reflection coefficient is

$$R_e(t) = -\frac{W_2'(t)/W_2(t) - q}{W_1'(t)/W_1(t) - q}, \quad (6)$$

where

$$q = -v \sqrt{1 - \eta^2/\eta^2},$$

and

$$\eta^2 = \epsilon_2 - i\mu_0 c^2 \sigma/\omega. \quad (7)$$

The relative permittivity of the earth is ϵ_2 and the conductivity is σ ; c is the speed of light and μ_0 is the permeability of free space.

Finally,

$$p(t) = \frac{W_2(t)W_1(t-y)}{W_1(t)W_2(t-y)}, \quad (8)$$

and

$$K \cong 11.96 I_0 l \sqrt{\frac{k}{a^3}} v^2, \quad (9)$$

where $I_0 l$ is the dipole current moment. In this paper, $I_0 l = 1$.

Equation (4) differs from that given by Wait [1961] only by the normalization, K , and the factor $(1+zt)^{5/2}$. Since $z \ll 1$, this factor is important only if $|t|$ is large. A quantitative discussion of its effect is given in section 3.

$$\text{If } |t| \ll v^2, (1+zt)^{5/2} \cong 1 + 5/2 zt. \quad (10)$$

Using the Wronskian [Spies and Wait, 1961],

$$W_1' W_2 - W_2' W_1 = 2i. \quad (11)$$

$$1 + R_e(t) = \frac{2i}{W_2(t)[W_1'(t) - qW_1(t)]}. \quad (12)$$

Then (4) is written

$$I_j = (-1)^{j-1} 4K e^{i\pi/4} \frac{e^{-ikd}}{\sqrt{\sin \theta}} \int_{\Gamma} (1+zt)^{5/2} e^{-ixt} \frac{E^{j-1}(t)F^j(t) dt}{C^{j+1}(t)}, \quad (13)$$

where

$$E(t) = W_2'(t) - qW_2(t), \quad (14)$$

$$F(t) = W_1(t-y)/W_2(t-y), \text{ and} \quad (15)$$

$$C(t) = W_1'(t) - qW_1(t). \quad (16)$$

The contour of integration has been discussed by Wait [1961] and Berry [1964]. The contour used for the numerical integration in this paper runs along the real axis from ∞ to the origin, and then into the third quadrant on a straight line with slope 1/4. In the third quadrant, the integrand gets small exponentially with $\exp(\text{Im}(tx))$, and on the real axis, when $t \gg 1$ [Spies and Wait, 1961],

$$\frac{1}{W_1(t)W_2(t)} \propto \exp\left(-\frac{4}{3}t^{3/2}\right), \quad (17)$$

so the integration need be carried out for only a finite portion of the contour in the vicinity of the origin.

2.1. The Saddle Point Approximation

The development here closely follows Wait [1961]. The difference is a small improvement in the accuracy of the approximations.

If $(-t) \gg 1$ [Olver, 1954],

$$W_k(t) \cong (-t)^{-1/4} \exp [(-1)^k i(\xi + \pi/4)] L[(-1)^k i\xi], \quad (18)$$

and

$$W_k'(t) \cong (-t)^{1/4} \exp [(-1)^k i(\xi - \pi/4)] M [(-1)^k i\xi], \quad (19)$$

where

$$\xi = \frac{2}{3}(-t)^{3/2}.$$

$$L(Z) = \sum_{j=0}^{\infty} U_j Z^{-j}, \text{ and } M(Z) = \sum_{j=0}^{\infty} V_j Z^{-j}, \quad (20)$$

where

$$U_0 = V_0 = 1, \text{ and}$$

$$U_j = \frac{(2j+1)(2j+3)\dots(6j-1)}{j!(216)^j}, \text{ and } V_j = -U_j \frac{6j+1}{6j-1}, j > 1. \quad (21)$$

Substituting (18) and (19) into (4),

$$I_j \cong e^{-i3\pi/4} K \frac{e^{-ikd}}{\sqrt{\sin \theta}} \int_{\Gamma} G(t) e^{-i\Omega(t)} dt, \quad (22)$$

where, letting $\alpha = (-t)^{1/2}$ and $s = \frac{2}{3}\alpha^3$,

$$G(t) = (1 - \alpha^2 z)^{5/2} \alpha^{-1} (1 + \hat{R})^2 \left(\frac{L(is)}{L(-is)} \hat{R} \right)^{j-1} L^2(is), \quad (23)$$

$$\Omega(t) = -x\alpha^2 + \frac{4}{3}j(y + \alpha^2)^{3/2} - \frac{4}{3}j\alpha^3, \text{ and} \quad (24)$$

$$\hat{R} = \frac{\alpha M(is) - iqL(is)}{\alpha M(-is) + iqL(-is)} \cdot \frac{L(-is)}{L(is)}. \quad (25)$$

The saddle point approximation for I_j is (compare Wait [1961])

$$I_j \cong e^{-i3\pi/4} K \frac{e^{-ikd}}{\sqrt{\sin \theta}} \left[\frac{2\pi}{i\Omega''(t_0)} \right]^{1/2} G(t_0) e^{i\Omega(t_0)}, \quad (26)$$

where t_0 is the saddle point found from

$$\alpha_0 = \frac{4j^2 y - x^2}{4xj} = (-t_0)^{1/2}. \quad (27)$$

Hence,

$$I_j \cong 2K e^{-i\pi/2} e^{-ikd} \sqrt{\frac{\pi}{x \sin \theta}} \left(1 + \frac{x}{2j\alpha_0} \right)^{1/2} (1 - \alpha_0^2 z)^{5/2} (1 + \hat{R})^2 \times \left[\frac{L(is_0)}{L(-is_0)} \hat{R} \right]^{j-1} L^2(is_0) e^{-i\Omega(t_0)}. \quad (28)$$

This reduces to Wait's [1961] result if L , M , and $(1 - \alpha^2 z)^{5/2}$ are set equal to one. As $\alpha \rightarrow \infty$, L and $M \rightarrow 1$; and as $\alpha \rightarrow 0$, $(1 - \alpha_0^2 z)^{5/2} \rightarrow 1$. Thus, the effect of retaining these factors is to increase the accuracy of (28) for extreme values of α . Quantitative results are shown in figure 2.

The reader is referred to Wait [1961] for a complete discussion of (28). He shows that $\left(1 + \frac{x}{2j\alpha_0} \right)^{1/2}$ is the convergence coefficient of geometric optics; $\Omega(t_0)$ is the difference between the electric length of the ray path and the distance along the earth; and R is the ground reflection coefficient. Thus, when $L = M = 1$, (28) multiplied by γ_j is the geometric-optics formula for the j th

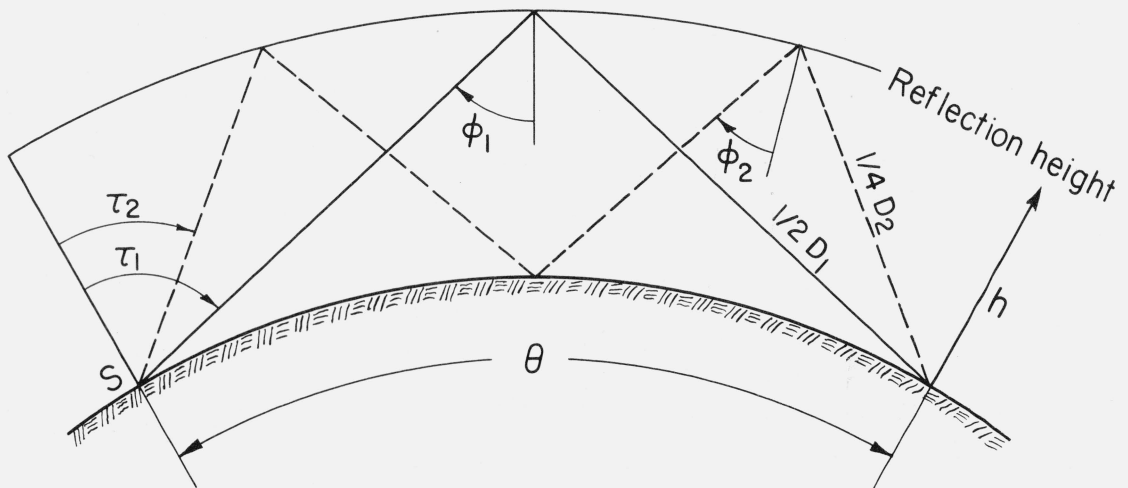


FIGURE 1. Geometry of first two wave hops.

ray hop. This justifies calling $\gamma_j I_j$ a "wave hop" and suggests using the concepts and terminology of geometric optics. Referring to figure 1, φ_j is the angle of incidence at the ionosphere of the j th hop, and τ_j is the angle of incidence at the ground. The ray path length of the j th hop is D_j . The region where $\tau_j < \pi/2$ is the lit region, $\tau_j = \pi/2$ is the caustic, and beyond the caustic is the shadow region.

Equation (27), and the condition $(-t) \gg 1$, show that (28) is valid only if d/j is sufficiently small, i.e., if $|\tau_j - \pi/2|$ is sufficiently large.

2.2. Residue Series for the Path Integrals

The integrand of (13) has poles of order $(j+1)$ at t_s if

$$W_1'(t_s) - qW_1(t_s) = 0. \quad (29)$$

The t_s are related to the poles, τ_s , of the Bremmer [1949] groundwave by [Wait and Conda, 1958]

$$t_s = \sqrt[3]{2} \tau_s. \quad (30)$$

Wait [1961] shows that these are the only poles, so I_j can be evaluated by summing a series of residues—at least in principle. The difficulty is the high order of the poles. Wait [1961] worked out the form of the residue for the first wave hop, but did not use it for calculations. Methods for calculating the residues of I_j , especially suitable for a digital computer, are given in this section.

Denote the residue at t_s of the integrand of I_j by $\text{Res}(j, t_s)$. Then

$$I_j \cong 8\pi i K e^{i\pi/4} \frac{e^{-ikd}}{\sqrt{\sin \theta}} \sum_{s=0}^{\infty} \text{Res}(j, t_s). \quad (31)$$

Rewrite (13) as

$$I_j = (-1)^{j-1} 4 e^{i\pi/4} K \frac{e^{-ikd}}{\sqrt{\sin \theta}} \int_{\Gamma} \frac{D(t) E^{j-1}(t) F^j(t)}{C^{j+1}(t)} dt = (-1)^{j-1} 4 e^{i\pi/4} K \frac{e^{-ikd}}{\sqrt{\sin \theta}} \int_{\Gamma} \frac{A_j(t)}{B_j(t)} dt, \quad (32)$$

where, using (10),

$$D(t) \cong (1 + 5/2zt) e^{-ixt} \quad (33)$$

Then

$$\text{Res}(j, t_s) = \frac{(-1)^j}{b_{j0}^{j+1}} \begin{vmatrix} a_{j0} & a_{j1} & a_{j2} & \dots & a_{jj} \\ b_{j0} & b_{j1} & b_{j2} & \dots & b_{jj} \\ 0 & b_{j0} & b_{j1} & \dots & b_{jj-1} \\ 0 & 0 & b_{j0} & \dots & b_{jj-2} \\ \cdot & \cdot & \cdot & \dots & \cdot \\ \cdot & \cdot & \cdot & \dots & \cdot \\ \cdot & \cdot & \cdot & \dots & \cdot \\ 0 & 0 & & b_{j0} & b_{j1} \end{vmatrix}, \quad (34)$$

$$\text{where } a_{jn}(t_s) = A_j^{(n)}(t_s)/n!, \text{ and } b_{jn}(t_s) = B_j^{(n+j+1)}(t_s)/(n+j+1)!. \quad (35)$$

The superscript (n) denotes the n th derivative. The determinant is easily evaluated numerically since it is nearly triangular.

Using Liebnitz's rule for the n th derivative of a product [Kaplan, 1952],

$$(gh)^{(n)} = \sum_{m=0}^n \frac{n!}{m!(n-m)!} g^{(m)} h^{(n-m)}, \quad (36)$$

the necessary derivatives of $[E(t)F(t)]$ and

$$A_j(t) = A_{j-1}(t)[E(t)F(t)] \quad (37)$$

are found recursively. This repetitive process is particularly appropriate for an electronic computer. The necessary derivatives of D , E , and F for the first five I_j are

$$D^{(n)}(t) = (-ix)^{n-1} e^{-ixt} \left[n \frac{5}{2} z - ix \left(1 + \frac{5}{2} zt \right) \right] \quad (38)$$

$$E'(t) = tW_2(t) - qW_2'(t),$$

$$E''(t) = tW_2'(t) + (1 - qt)W_2(t),$$

$$E^{(3)}(t) = (t^2 - q)W_2(t) + (2 - qt)W_2'(t), \quad (39)$$

$$E^{(4)}(t) = (4t - qt^2)W_2(t) + (t^2 - 2q)W_2'(t), \text{ and}$$

$$E^{(5)}(t) = (4 - 4qt + t^3)W_2(t) + (6t - qt^2)W_2'(t),$$

$$F'(t) = 2i[W_2(t - \gamma)]^{-2},$$

$$F''(t) = -2GF'(t),$$

$$F^{(3)} = \{-2(t - \gamma) + 6G^2\}F'(t) \quad (40)$$

$$F^{(4)}(t) = \{-2 + 16(t - \gamma)G - 24G^3\}F'(t), \text{ and}$$

$$F^{(5)}(t) = \{16(t - \gamma)^2 + 20G - 120(t - \gamma)G^2 + 120G^4\}F'(t).$$

In (40), $G = W_2'(t - \gamma)/W_2(t - \gamma)$.

The b_{jn} can be found by repeated use of (36) and (26), but are given explicitly here for the first five hops:

$$\begin{aligned} b_{j0} &= (C'(t_s))^{j+1}, j = 1, \dots, 5 \quad b_{j1} = \frac{j+1}{2} (C'(t_s))^j C''(t_s), j = 1, \dots, 5 \\ C'(t_s)b_{j2} &= \frac{j}{4} C''(t_s)b_{j1} + \frac{j+1}{6} C^{(3)}(t_s)b_{j0}, j = 2, \dots, 5 \\ C'(t_s)b_{j3} &= \frac{j-1}{6} C''(t_s)b_{j2} + \frac{2j+1}{18} C^{(3)}(t_s)b_{j1} + \frac{j+1}{24} C^{(4)}(t_s)b_{j0}, j = 3, 4, 5 \end{aligned} \quad (41)$$

$$\begin{aligned}
C'(t_s)b_{j4} &= \frac{j-2}{8} C''(t_s)b_{j3} + \frac{j}{12} C^{(3)}(t_s)b_{j2} + \frac{3j+2}{96} C^{(4)}(t_s)b_{j1} + \frac{j+1}{120} C^{(5)}(t_s)b_{j0}, \quad j=4, 5 \\
b_{55} &= \frac{3}{16} C'(t_s) (C''(t_s))^5 + \frac{5}{4} (C'(t_s))^2 (C''(t_s))^3 C^{(3)}(t_s) \\
&\quad + \frac{5}{6} (C'(t_s))^3 C''(t_s) (C^{(3)}(t_s))^2 + \frac{5}{8} (C'(t_s))^3 (C''(t_s))^2 C^{(4)}(t_s) \\
&\quad + \frac{5}{24} (C'(t_s))^4 C^{(3)}(t_s) C^{(4)}(t_s) + \frac{1}{8} (C'(t_s))^4 C''(t_s) C^{(5)}(t_s) + \frac{1}{120} (C'(t_s))^5 C^{(6)}(t_s).
\end{aligned}$$

The function $C(t)$ differs from $E(t)$ only by the index on the Airy functions, so using (29) and (39) the necessary derivatives of $C(t_s)$ are

$$\begin{aligned}
C'(t_s) &= (t_s - q^2)W_1(t_s), \\
C''(t_s) &= W_1(t_s), \\
C^{(3)}(t_s) &= (t_s^2 - q^2 t_s + q)W_1(t_s), \\
C^{(4)}(t_s) &= (4t_s - 2q^2)W_1(t_s), \\
C^{(5)}(t_s) &= (t_s^3 - q^2 t_s^2 + 2t_s q + 4)W_1(t_s), \text{ and} \\
C^{(6)}(t_s) &= (9t_s^2 - 6q^2 t_s + 6q)W_1(t_s).
\end{aligned} \tag{42}$$

Before the convenient form of (34) and the recursive method of (36) and (37) were noticed, explicit expressions for $\text{Res}(j, t_s)$, $j=1, \dots, 5$, were derived and programmed. To appreciate the economy of (34) and (37), note that $\text{Res}(5, t_s)$ is the sum of 18 distinct terms, and one factor of one of these terms, a_{55} , is the sum of 73 distinct terms.

3. Sample Calculations and Discussion

An efficient program for calculating the path integrals must use all three methods given above. The saddle point approximation should be used whenever possible because it is simplest; but it is not valid near, or beyond, the caustic. The residue series is accurate and efficient deep in the shadow region, but converges very slowly in the lit region. If these two methods do not overlap in the caustic region, (13) must be integrated numerically.

The three methods of calculating the path integrals were compared by computing I_j , $j=1, \dots, 5$, as a function of distance, $d=1000, \dots, 8000$ km, for 10 kc/s, 100 kc/s, and 1000 kc/s. The regions of validity of the methods overlap enough to lend confidence to the computer routines and to allow a program to automatically select the appropriate method. Two examples which illustrate the comparisons are shown in figure 2. For all calculations in this paper, $\epsilon_2=15$. The solid line indicates I_j , the other lines show the departure from I_j of the various formulas. The simpler saddle point approximation given by Wait [1961] has also been plotted. The caustic is indicated by an arrow. Figure 2a shows I_2 (100 kc/s). There is a small difference between the value and the simple form of the saddle point approximation near 1000 km. The numerical integration also departs from the value here, but this could have been avoided with a higher order quadrature. Between 2000 km and 3000 km the error becomes very large in both the saddle point approximation and residue series, so numerical integration is necessary. Beyond 6000 km, the numerical integration becomes inaccurate.

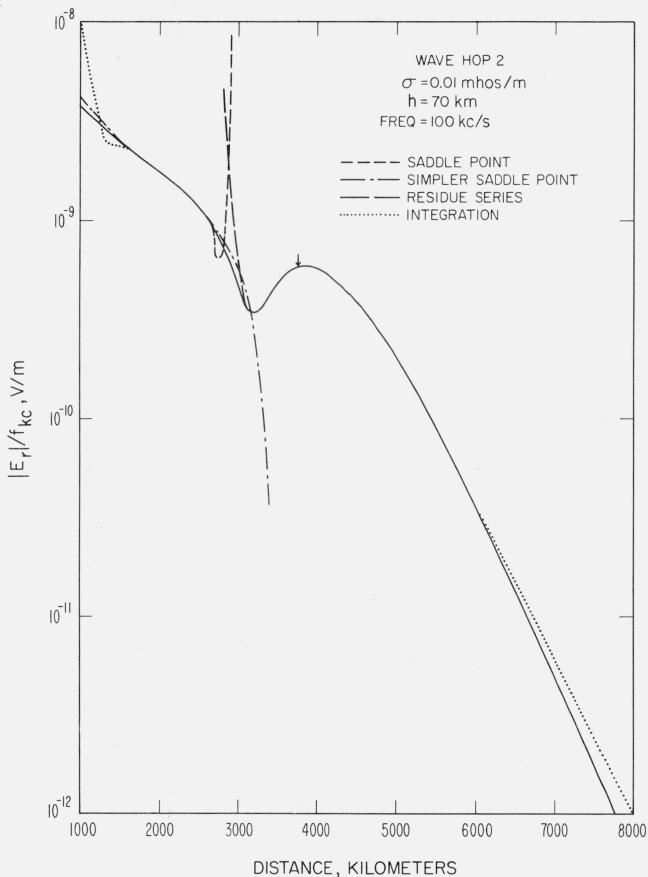


FIGURE 2a. Comparison of various methods of calculation, I_2 (100 kc/s).

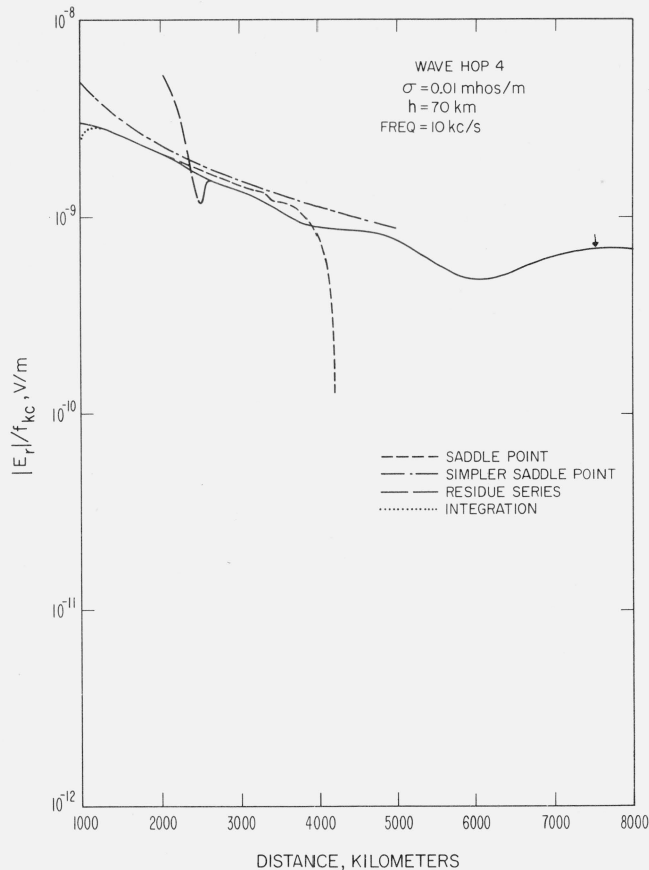


FIGURE 2b. Comparison of various methods of calculation, I_4 (10 kc/s).

Figure 2b shows I_4 (10 kc/s). For this case, only a small error would result between 2000 km and 3000 km from using only the saddle point approximation and the residue series. The simple form of the saddle point approximation is not as accurate for 10 kc/s as for 100 kc/s. The error is increasing near 1000 km. This is because α_0 is large here, so the approximation, $(1 - \alpha^2 z)^{5/2} \cong 1$, used by Wait [1961], is not valid in this region. However, in most practical applications, the 4th hop is insignificant at this distance.

Graphical presentation of the phase of I_j is impractical because it varies rapidly with distance. Instead, a phase lag, relative to the free space ray path, is defined. Let $-\pi < [A] \leq \pi$ denote an angle equivalent to A —i.e., $[A]$ differs from A by an integral multiple of 2π . Then, the path integral phase lag, β , is defined by

$$\beta_j = -\{[\text{phase } I_j] + [kD_j] + \pi/2\}. \quad (43)$$

Since $\Omega(t_0) \cong k(d - D_j)$ [Wait, 1961], (25) shows that, for perfectly conducting earth ($R \equiv 1$), $[\text{phase } I_j] \cong -\frac{\pi}{2} - [kd] - [kD_j - d] \cong -[kD_j] - \frac{\pi}{2}$ in the saddle point approximation. Thus β_j is generally small and varies slowly in the lit region.

Figures 3, 4, and 5 show the amplitude and phase lag of the first 3 path integrals as a function of distance for frequencies from 10 kc/s to 200 kc/s. (Note that the amplitude has been divided by the frequency in kilocycles.) For the 70-km reflection height, the first hop caustic is at $d \cong 1880$ km. Figure 3a shows the diffraction of the first hop into the shadow region. As would be expected, the lower frequencies diffract further into the shadow region than the higher frequencies. The phase lag of I_1 is shown in figure 3b. The exponential decrease of the amplitude and the linear increase of the phase lag deep in the shadow region confirm the groundwavelike behavior of the wave hop beyond the caustic predicted by Wait [1961].

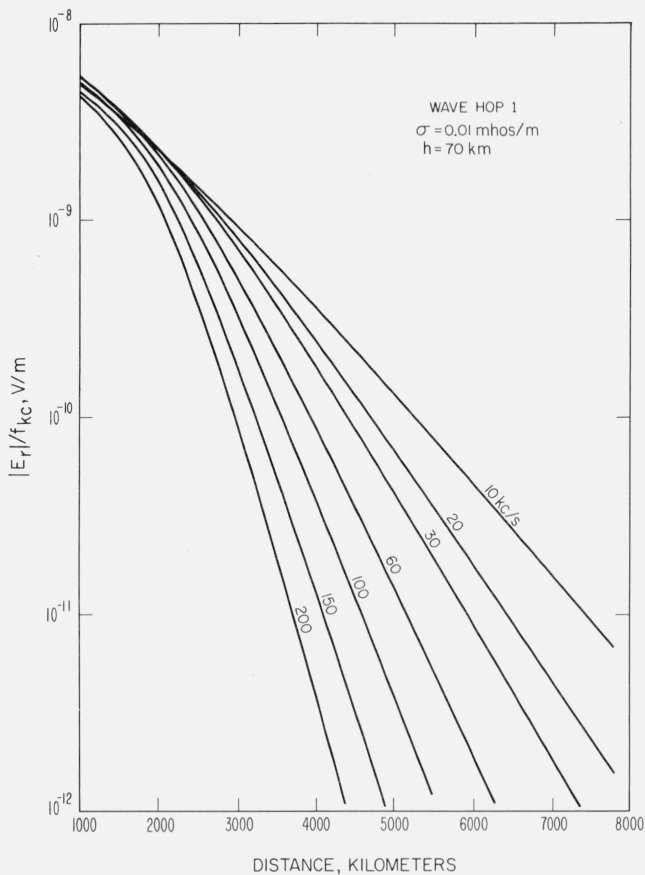


FIGURE 3a. Amplitude of I_1 as a function of distance.

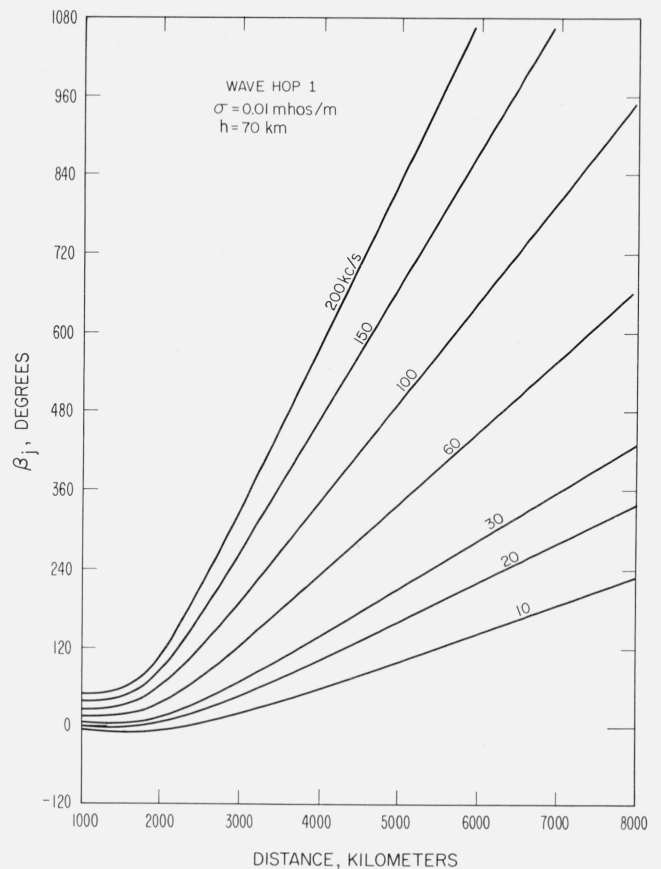


FIGURE 3b. Phase lag of I_1 as a function of distance, showing diffraction into the shadow region.

Figure 4 shows the amplitude and phase lag of I_2 . The relative minimum in the amplitude between 2000 km and 3000 km is caused by the pseudo-Brewster angle in the ground reflection coefficient [Bremmer, 1949; Berry, 1964]. The sharpest minimum is for a frequency of 150 kc/s. Figure 4b shows the change in the phase lag corresponding to the minimum in the amplitude curve. For 150 kc/s there is a rapid phase shift of 180° corresponding to the sharp minimum in the amplitude curve. The frequency dependence of the pseudo-Brewster angle is clearly shown in figure 4a. The pseudo-Brewster angle is also shown in the amplitude and phase lag of I_3 in figures 5a and 5b.

The present computer program can calculate I_4 and I_5 but no examples are shown here, since no new phenomena occur. Finally, the calculation is not limited to the frequencies shown—a test case at 10 Mc/s ran successfully.

4. Examples of Applications

Equation (1) shows that the path integrals are the natural complements of ionospheric reflection coefficients. Reflection coefficients have been calculated and published for a variety of theoretical models of the ionosphere, e.g., Jöhler, Walters, and Harper [1960], Jöhler and Harper [1962], Wait and Walters [1963a, 1963b, 1963c] and Walters and Wait [1963]. Using these, or any other reflection coefficients, and graphs of the path integrals, such as figures 3, 4, and 5, theoretical LF and VLF field strengths can be calculated quickly and easily by hand.

For example, Wait and Walters [1963a] show that VLF reflection coefficients for an exponential ionosphere are given approximately by $|T| \cong \exp(-A \cos \varphi_j)$ for some constant A . In

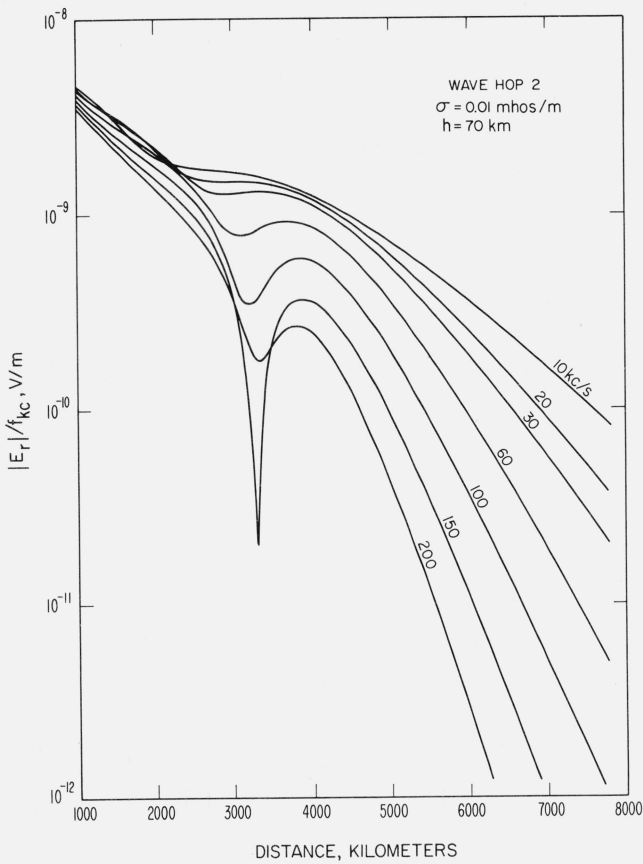


FIGURE 4a. Amplitude of I_2 as a function of distance, showing the pseudo-Brewster angle near 3000 km.

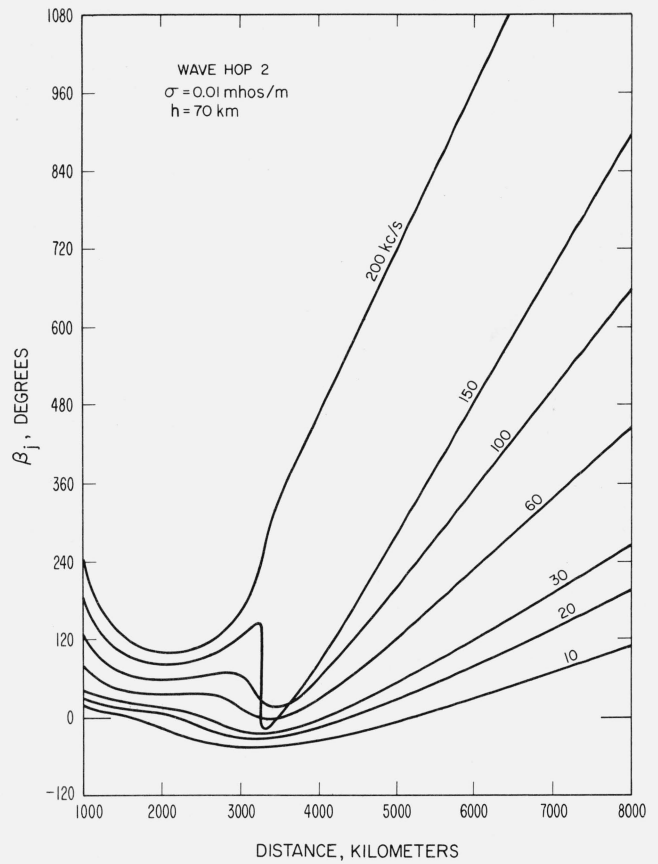


FIGURE 4b. Phase lag of I_2 as a function of distance.

particular, for a frequency of 20 kc/s, and a reasonable choice of parameters, they find $A \cong 3$. $\cos \varphi_j$ is given exactly by [Bremmer, 1949]:

$$\cos \varphi_j = \left[a \left(1 - \cos \frac{\theta}{2j} \right) + h \right] \left[2a(a+h) \left(1 - \cos \frac{\theta}{2j} \right) + h^2 \right]^{-1/2} \quad (44)$$

If $jh/d \ll 1$

$$\cos \varphi_j \cong \sqrt{\frac{h}{a} + 4 \left(\frac{jh}{d} \right)^2}. \quad (45)$$

With this model ionosphere, and the information in figures 3, 4, and 5, the amplitudes of the first three wave hops were calculated and are shown in figure 6. The total field could also be found by calculating the phases and summing. The sum should include the groundwave at distances less than about 1000 km.

The path integrals can also be used to remove the effects of the earth's conductivity, diffraction loss, etc., from experimental data. In figure 7, monthly averages of 100-kc/s first-hop skywave amplitudes are shown as a function of GMT for a 2510-km path from Attu to Sitkinak in the Aleutians [Doherty, 1964]. These are Loran-C pulse measurements, so the groundwave could be measured before the first-hop skywave arrived. The ordinate scale is $A = 20 \log_{10} (E_1/E_0) + 12$.

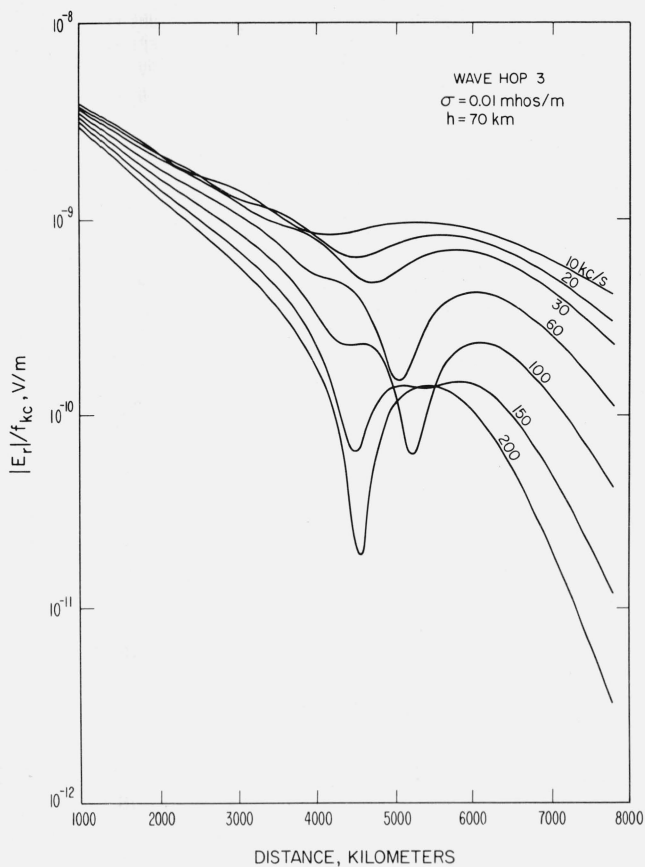


FIGURE 5a. Amplitude of I_3 as a function of distance.

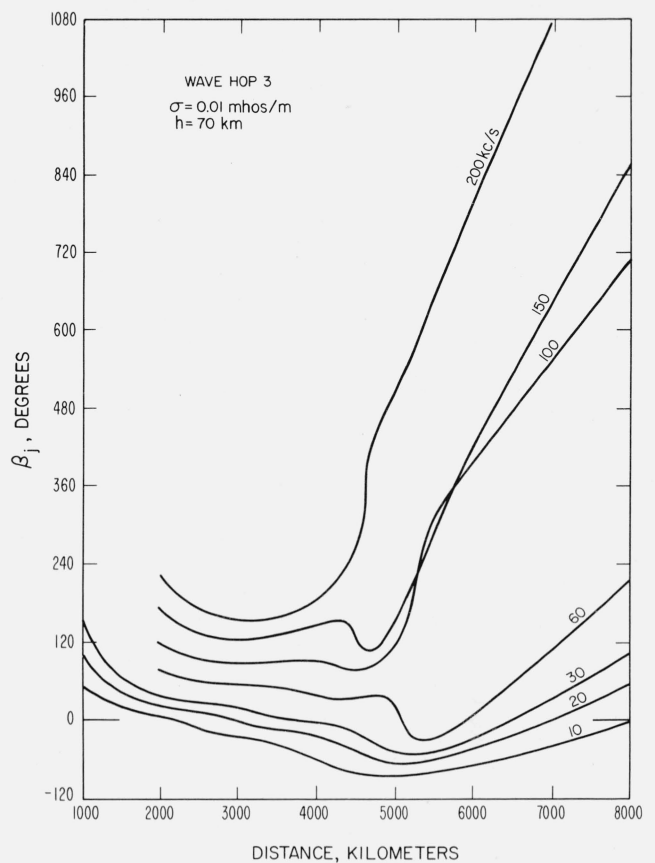


FIGURE 5b. Phase lag of I_3 as a function of distance.

Since $E_1 = TI_1$, the ionospheric reflection coefficient is given by

$$\log_{10} T = \frac{A-12}{20} - \log_{10} \frac{I_1}{E_0}. \quad (46)$$

The ratio of the first path integral to the groundwave was calculated for reflection heights of 65 km (daytime reflection height) and 85 km (nighttime reflection height), for a sea path. These ratios are 217.4 and 295.3, respectively. With these ratios, and (46), the measurements in figure 7 can be converted directly to reflection coefficient magnitudes, without making assumptions about the antenna pattern or transmitter power. Note, however, that the reflection coefficient is dependent on the assumed reflection height and the assumed ground constants. For example, in September 1962, the average grazing reflection coefficient during the day for this path ranged from 0.013 to 0.018, and was about 0.07 for several hours during the night.

5. Concluding Remarks

The major barrier to practical use of the wave hop theory has been the difficulty of calculating the path integrals near the caustic and in the shadow region. The necessary formulas for such calculations are given in this paper and sample calculations are shown illustrating the general characteristics of the path integrals. The path integrals can be used in conjunction with published values of reflection coefficients to calculate theoretical LF, VLF fields by hand, or they can be used to extract reflection coefficients from experimental data. Therefore, the path integrals are being calculated as a function of distance for seven frequencies from 10 kc/s to 200 kc/s, for reflection heights from 60 km to 100 km, for sea water paths, and for land paths with conductivity 0.01 and 0.001 mhos/m, and will be published soon [Berry and Chrisman, 1965].

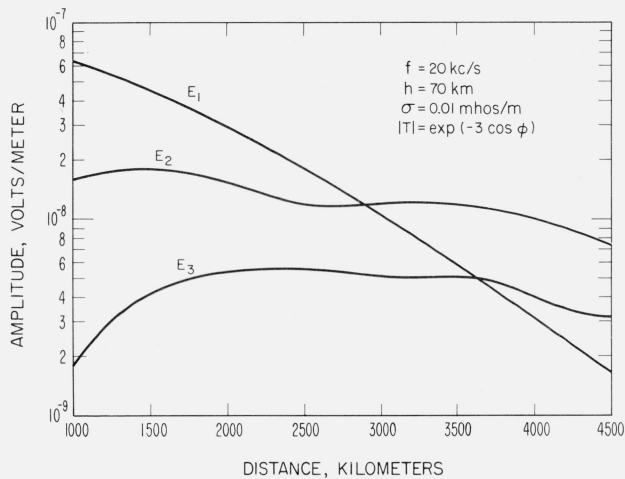


FIGURE 6. Sample calculation of amplitude of first three hops, using figures 3, 4, and 5, $f = 20 \text{ kc/s}$, $|T| = \exp(-3 \cos \phi)$.

TYPICAL AMPLITUDE CURVES FOR SITKINAK VERSUS HOUR OF DAY AND VERSUS ZENITH ANGLE OF THE SUN

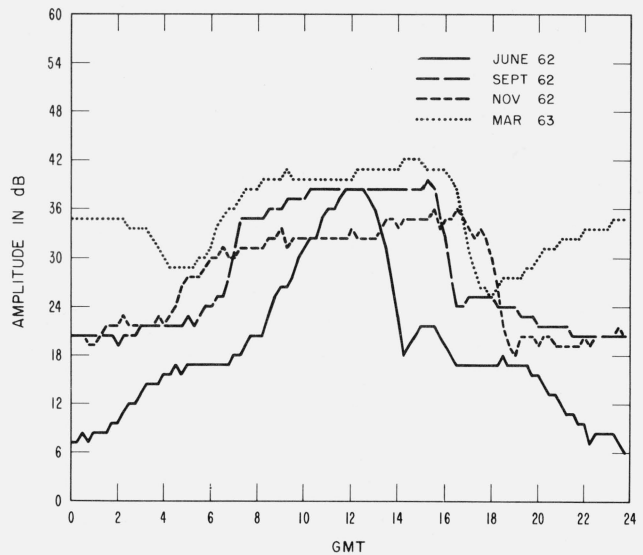


FIGURE 7. Measured first-hop skywaves relative to groundwave, $f = 100 \text{ kc/s}$ [after Doherty, 1965].

6. References

- Berry, L. A. (1964), Wave hop theory of long distance propagation of low frequency radio waves, *Radio Sci. J. Res. NBS* **68D**, No. 12, 1275-1284.
- Berry, L. A., and M. E. Chrisman (1965), Numerical values of the path integrals for low and very low frequencies, *NBS Tech. Note No. 319*.
- Bremmer, H. (1949), *Terrestrial Radio Waves* (Elsevier Publishing Co., New York, N.Y.).
- Doherty, R. H. (1964), Low frequency propagation at high latitude. Paper presented at the Spring 1964 URSI Meeting, Washington, D.C.
- Fock, V. A. (1946), *Diffraction of Radio Waves Around the Earth's Surface* (Publishers of the Academy of Science, Moscow, USSR).
- Johler, J. R., and J. D. Harper, Jr. (1962), Reflection and transmission of radio waves at a continuously stratified plasma with arbitrary magnetic induction, *J. Res. NBS* **66D** (Radio Prop.), No. 1, 81-99.
- Johler, J. R., L. C. Walters, and J. D. Harper, Jr. (1960), Low- and very-low-frequency model ionosphere reflection coefficients, *NBS Tech. Note No. 69*.
- Kaplan, W. (1952), *Advanced Calculus* (Addison-Wesley Publishing Co., Inc., Reading, Mass.).
- Olver, F. W. J. (1954), The asymptotic expansion of Bessel functions, *Phil. Trans. Roy. Soc. London, Ser. A* **247**, 364-367.
- Rydbeck, O. E. H. (1944), On the propagation of radio waves, *Trans. Chalmers Univ. of Technol.* **34**.
- Spies, K. P., and J. R. Wait (1961), Mode calculations for VLF propagation in the earth-ionosphere waveguide, *NBS Tech. Note No. 114*.
- Wait, J. R. (1961), A diffraction theory of LF sky-wave propagation, *J. Geophys. Res.* **66**, No. 6, 1713-1724.
- Wait, J. R., and A. M. Conda (1958), Pattern of an antenna on a curved lossy surface, *IRE Trans. Ant. Prop.* **AP-6**, No. 4, 348-359.
- Wait, J. R., and A. M. Conda (1961), A diffraction theory of LF skywave propagation—an additional note, *J. Geophys. Res.* **66**, No. 6, 1725-1729.
- Wait, J. R., and L. C. Walters (1963a), Reflection of VLF radio waves from an inhomogeneous ionosphere. Part I. Exponentially varying isotropic model, *J. Res. NBS* **67D** (Radio Prop.), No. 3, 361-367.
- Wait, J. R., and L. C. Walters (1963b), Reflection of VLF radio waves from an inhomogeneous ionosphere. Part II. Perturbed exponential model, *J. Res. NBS* **67D** (Radio Prop.), No. 5, 519-523.
- Wait, J. R., and L. C. Walters (1963c), Reflection of VLF radio waves from an inhomogeneous ionosphere. Part III. Exponential model with hyperbolic transition, *J. Res. NBS* **67D** (Radio Prop.), No. 6, 747-752.
- Walters, L. C., and J. R. Wait (1963), Numerical calculations for reflection of electromagnetic waves from a lossy magneto plasma, *NBS Tech. Note No. 205*.

(Paper 69D11-580)